THE ASTROPHYSICAL JOURNAL, 301:664–674, 1986 February 15

THE STRUCTURE OF THE SMALL MAGELLANIC CLOUD

D. S. MATHEWSON, V. L. FORD, AND N. VISVANATHAN
Mount Stromlo and Siding Spring Observatories, Australian National University
Received 1985 June 7; accepted 1985 August 19

ABSTRACT

In velocity-space there appear to be two separate entities in the H I distribution in the SMC, each with its own stellar and nebular populations. In an attempt to delineate the geometry of these two entities, *B*, *V*, and near-infrared photometry was done for 161 Cepheids in the SMC to derive their relative distances to an accuracy of $\pm 4\%$ (about ± 3 kpc at the distance of the SMC). The Cepheids extend from ~ 43 to 75 kpc with a maximum concentration at 59 kpc. This depth of 32 kpc is much greater than the 5 kpc anticipated on the basis of the areal distribution of Cepheids over the main body of the SMC. The line-of-sight distribution of the younger Cepheids with periods greater than 10 days (for which there is almost a complete sample) splits into two components, each of depth of about 6 kpc and with centers 12 kpc apart. The central zone is deepest with an extension to almost 90 kpc. Recent radial velocity measurements of stars and their interstellar Ca II absorption lines show convincingly that the near and far components should be identified with the low- and high-velocity entities respectively. The results are in good agreement with the "tidal" model of Murai and Fujimoto, which has the SMC colliding with the LMC 2×10^8 yr ago. This close encounter with the LMC plus the recent perigalactic passage appears to be stripping the SMC of much of its mass, and it is in the process of irreversible disintegration.

Subject headings: galaxies: internal motions — galaxies: Magellanic Clouds — galaxies: structure — photometry — radio sources: 21 cm radiation — stars: Cepheids

I. INTRODUCTION

From an analysis of the radial velocities of the neutral hydrogen, stars, and emission nebulae in the Small Magellanic Cloud, Mathewson and Ford (1984) and Mathewson (1984) propose that the SMC was torn in half by a very close encounter with the LMC some 2×10^8 yr ago (Murai and Fujimoto 1980). In velocity-space, there appear to be two separate entities in the H I, each with its own stellar and nebular populations. The fragment with the lower radial velocity is identified with the Small Magellanic Cloud Remnant (SMCR), and the one with the higher radial velocity is named the Mini-Magellanic Cloud (MMC).

In an attempt to spatially separate these two masses, distance measurements of 161 Cepheids were made using the most accurate known method, i.e., the period-luminosity relation in the infrared. McGonegal *et al.* (1982, 1983) have demonstrated that infrared photometry of Cepheids overcomes uncertainties due to interstellar extinction, the dependence of the P-L relation on color or amplitude, and the effects of variations in chemical composition between galaxies. Their method has been further refined by Welch and Madore (1984) and Visvanathan (1985) by reducing random phase observations to mean light. Where possible, this procedure has been used in this paper. While absolute distances to the Cepheids are derived by using Galactic Cepheids to establish the zero point of the distance scale, relative distances are the most important parameter in this particular exercise. It is believed that these have been determined to an accuracy of about 4%, i.e., to better than 3 kpc at the distance of the SMC.

II. OBSERVATIONS AND REDUCTIONS

a) Sample Selection

The Cepheids were selected from the catalogs of Payne-Gaposchkin and Gaposchkin (1966), Gascoigne (1979), Butler (1976) and Martin (1980). The selection criteria were that (*a*) complete light curves existed, so that anomalous and type II Cepheids could be avoided; (*b*) where possible, photoelectric or accurate photographic mean light *V* magnitudes $\langle V \rangle$ were available, so that the random phase infrared measurements could be corrected to mean light; (*c*) they were fairly uniformly distributed over the main body and bridge of the SMC; (*d*) the Cepheids did not lie in the direction of the dark nebulae in the central Bar listed by Hodge (1974); (*e*) as complete a sample as possible be obtained for Cepheids of period greater than 10 days, as these are most representative of extreme Population I; (*f*) and as many shorter period Cepheids as possible be measured to reveal any age effect.

A total of 161 Cepheids was observed, and the positions of 153 of them are shown on the photograph of the SMC in Figure 1. Eight of them are too far to the east to appear on the photograph.

b) Photometric Procedures

The photometric observations in the I_V (1.05 μm), *V* (5500 Å), and *B* (4500 Å) wavebands were carried out at the Cassegrain foci of the 1 m, 2.3 m, and 3.9 m (AAT) telescopes at Siding Spring Observatory using the automatic scanner in the chopping mode (Visvanathan 1983, 1985). A Varian photomultiplier tube with an InGaAsP cathode was operated at 2000 V at the dry ice temperature. Pulse counting was used in all the observations, and sufficient counts were obtained from each Cepheid to reach an accuracy of 3% in I_V. The exposure times for I_V, *V*, and *B* filters are 4.5, 1.13, and 1.13 s for a single rotation.

The sky for the sky aperture was chosen carefully from the acquisition television image of the field, and the instrument was rotated to acquire it. The TV system was integrated sufficiently so that only stars 5 mag or more fainter than the

1986ApJ...301..664M

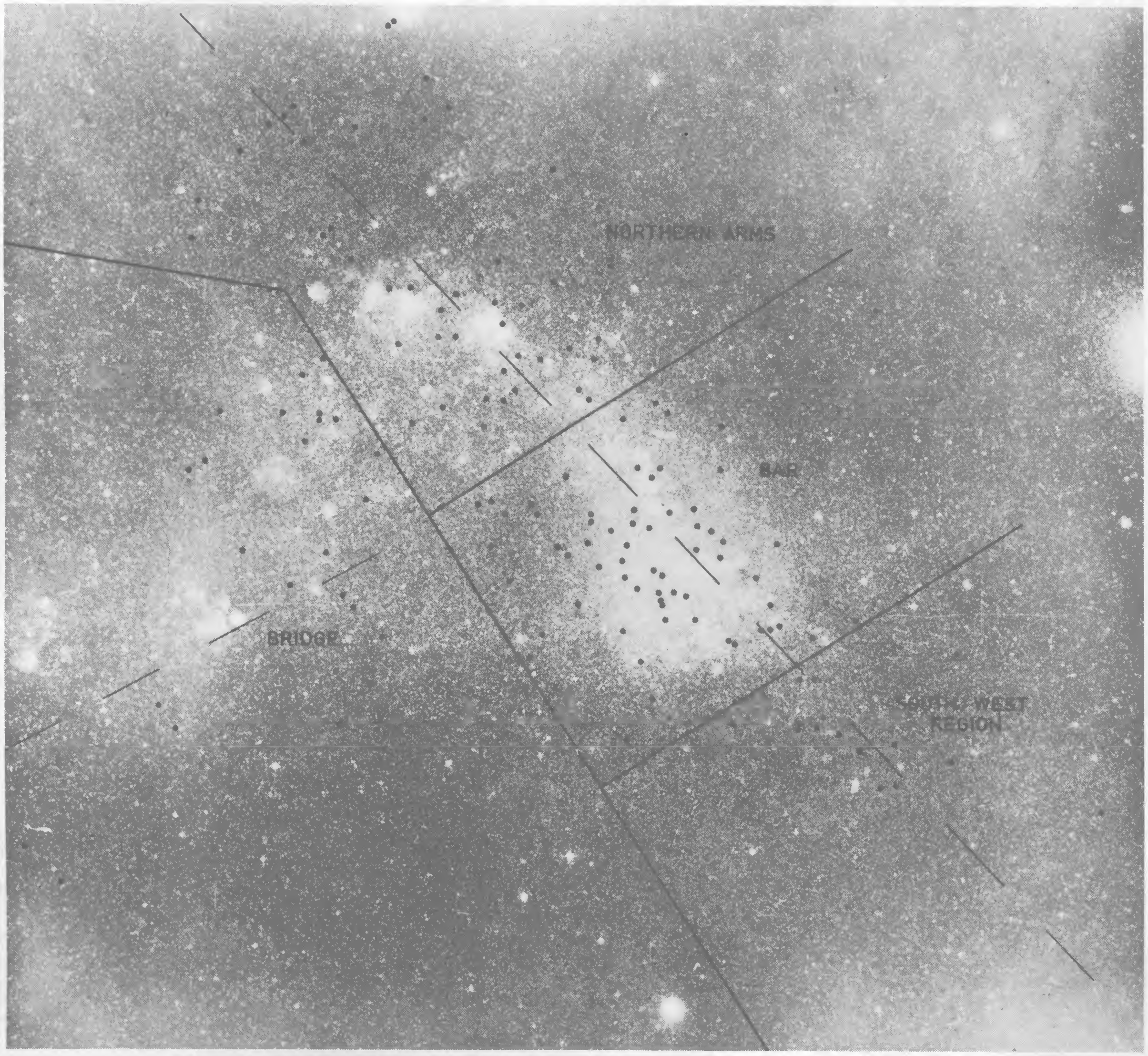

FIG. 1.—The areal distribution of 153 of the 161 Cepheids observed in the SMC. The eight others are off the photograph to the east. The SMC is divided into the subsystems defined on the map, and the major axis and ridge line of the Bridge are shown as broken lines.

Cepheid lay in the sky aperture. All the observations were done during excellent photometric and seeing conditions. To overcome the sensitivity differences between the sky and the star apertures, two observations were made one after the other: one centering the star in the star aperture, and another centering the star in the sky aperture. The sky-subtracted counts from both the observations were added and converted into magnitude and reduced to outside the atmosphere using the average extinction coefficient. Local standard stars were observed often to monitor extinction and instrumental changes. These standards were tied to the E region standards (Vogt, Geisse, and Rofas 1981; Graham 1982). The zero point of the V scale was set equal to that of the UBV system, and that of the color indices $V-I_V$ and $B-V$ were set equal to zero for AO V stars.

c) Data

Table 1 lists the data for the 161 Cepheids observed in the SMC.

Columns (1) and (2).—The Cepheid name and its period.

Column (3).—The telescope used is indicated by the numbers 1, 2, and 3 representing the 1 m, 2.3 m, and 3.9 m (AAT) telescopes at Siding Spring Observatory respectively.

Column (4).—The Julian date of observation.

Column (5).—The V magnitude at mean light. The 85 photoelectric values (mean error $0^m.03$) of $\langle V \rangle$ are taken from Caldwell and Coulson (1984), while the 47 photographic values, denoted by superscript "a," are the mean of the $\langle V \rangle$ magnitudes given by Martin (1980) and Butler (1976). Martin and Butler have 43 and 21 Cepheids in common with the photoelectric data respectively, and their dispersion computed from the differences is $0^m.1$.

Columns (6)–(8).—The observed V, $B-V$, and I_V magnitudes respectively.

Column (9).—The infrared magnitude at mean light computed by adding to I_V the quantity $(\langle V \rangle - V)/3$. The ratio of the amplitudes of the light curves at V and I_V is taken as 3 (Wisniewski and Johnson 1968). The mean error in $\langle I_V \rangle$ is about $0^m.04$.

Column (10).—The infrared magnitude at mean light corrected for reddening. A value of $0^m.06$ (Caldwell and Coulson 1985) has been subtracted from $\langle I_V \rangle$ to correct for the effects of interstellar absorption (see § II*d*). The mean error in $\langle I_V \rangle_0$ is about $0^m.05$.

Column (11).—The distances of the Cepheids in the SMC.

TABLE 1

B, *V*, AND I_V OBSERVATIONS OF SMC CEPHEIDS

HV. (1)	P. (days) (2)	Tel. (3)	J. D. 2440000+ (4)	<V> (5)	V (6)	(B−V) (7)	I_V (8)	$\langle I_V \rangle$ (9)	$\langle I_V \rangle_0$ (10)	Dist. (Kpc) (11)	R. A. (1950) h. m. s. (12)	Dec. (1950) ° ′ ″ (13)
1907	1.643	3	5603.227	16.92[a]	17.35		16.46	16.32	16.26	62	01 00 47.8	-71 36 00
1796	1.960	3	5989.182	17.25[a]	17.22	0.55	16.09	16.10	16.04	65	00 57 47.0	-72 42 58
		3	5989.218		17.22	0.43	16.34	16.35	16.29			
1869	2.464	3	5684.047	17.04	16.90		15.88	15.93	15.87	65	00 59 34.3	-71 33 31
1726	2.636	3	5989.067	15.98	15.95	0.41	15.24	15.25	15.19	49	00 56 31.5	-73 26 52
2015	2.874	3	5684.033	16.43	16.55		15.51	15.47	15.41	58	01 04 18.2	-71 37 24
1906	3.066	3	5684.004	16.27	16.42		15.48	15.43	15.37	59	01 00 40.4	-71 26 16
2037	3.368	3	5988.962	15.39[a]	15.52	0.57	14.49	14.45	14.39	39	01 06 25.4	-73 48 06
1339	3.489	3	5989.088	16.41[a]	16.74	0.84	15.43	15.32	15.26	60	00 37 07.7	-73 33 20
1783	3.655	2	5994.237		15.57	0.69	14.41			41:	00 57 09.4	-72 10 33
1804	3.666	3	5988.942	15.50[a]	15.20	0.32	14.64	14.74	14.68	47	00 57 57.6	-72 49 16
212	3.899	3	5683.973	15.85	16.32		15.17	15.01	14.95	56	01 01 39.6	-71 12 09
1694	3.934	3	5989.050		16.08	0.67	15.11			58:	00 54 57.0	-73 10 43
1653	3.972	3	5989.031		16.26	0.66	15.25			63:	00 53 49.8	-73 18 28
214	4.207	3	5683.987	15.66	15.52		14.78	14.83	14.77	53	01 02 29.3	-71 13 28
1425	4.547	3	5684.124	15.93[a]	15.53		15.03	15.16	15.10	65	00 44 59.6	-72 48 58
1537	5.842	2	6027.885	15.60[a]	15.64	0.36	15.01	15.00	14.94	70	00 49 48.2	-74 04 52
10375	5.938	2	6032.064	15.80[a]	15.75	0.71	14.70	14.72	14.66	62	01 07 21.5	-71 31 55
1500	5.949	2	6027.949	15.80[a]	15.98	0.65	15.11	15.05	14.99	72	00 48 27.2	-73 54 10
2203	5.962	2	6025.249	15.70[a]	15.28	0.42	14.63	14.77	14.71	64	01 12 53.1	-72 02 13
2124	6.064	2	6029.149	15.47[a]	15.96	0.86	14.74	14.58	14.52	59	01 07 49.7	-71 34 11
2198	6.064	2	6029.195	15.61[a]	15.63	0.61	14.78	14.77	14.71	64	01 12 24.3	-71 53 12
2040	6.112	2	6006.236	15.41[a]	15.43	0.58	14.58	14.57	14.51	59	01 05 52.3	-72 47 21
1612	6.182	2	6025.155	15.33[a]	15.42	0.73	14.53	14.50	14.44	57	00 52 42.9	-73 32 09
1492	6.292	3	5684.141	15.26	14.84		14.00	14.13	14.07	49	00 48 37.9	-72 44 02
1979	6.296	2	5994.088	15.12[a]	15.37	0.62	14.39	14.31	14.25	53	01 03 35.0	-72 56 11
1520	6.384	2	6025.108		15.96	0.75	14.83			68:	00 49 29.6	-72 59 55
11193	6.427	2	6031.018	15.78[a]	15.70	0.62	14.71	14.74	14.68	66	00 59 19.2	-72 17 59
2174	6.429	2	5994.052	15.04[a]	14.82	0.60	13.78	13.85	13.79	44	01 10 09.2	-71 42 11
1412	6.463	2	6004.947	15.84[a]	16.12	1.05	15.06	14.97	14.91	73	00 43 44.7	-73 59 52
		2	6032.012		16.21	0.80	15.08	14.96	14.90			
2142	6.490	2	6026.140	15.52[a]	15.26	0.49	14.52	14.61	14.55	59	01 08 38.8	-71 36 02
		2	6029.107		15.42	0.61	14.41	14.44	14.38			
1512	6.546	2	6031.173		16.00	0.90	14.90			71:	00 49 02.3	-73 45 30
1988	6.561	2	5998.233	15.40[a]	15.35	0.64	14.30	14.32	14.26	55	01 04 28.0	-73 51 08
11112	6.611	2	6030.936	15.65	15.75	0.70	14.67	14.64	14.58	64	00 21 56.9	-74 13 04
2163	6.693	2	6005.133	15.59[a]	15.41	0.53	14.50	14.56	14.50	62	01 11 12.7	-73 17 45
2054	7.165	2	6030.963	15.30[a]	15.32	0.66	14.35	14.34	14.28	58	01 05 46.1	-72 01 47
1527	7.228	2	6026.103		16.12	1.17	14.67			62:	00 49 39.1	-73 13 01
		2	6029.079		15.03	0.44	14.25					
2119	7.272	2	6032.117	15.48[a]	15.55	0.70	14.51	14.49	14.43	63	01 08 42.5	-72 45 19
1427	7.334	2	6030.989		16.14	0.77	14.89			76:	00 44 49.5	-73 20 08
853	7.334	2	6006.086	14.86[a]	14.84	0.54	13.96	13.97	13.91	50	01 04 09.6	-73 56 11
1548	7.350	2	6006.196	15.31[a]	15.75	0.70	14.63	14.48	14.42	63	00 50 18.2	-72 47 35
1973	7.480	2	5996.195	15.37[a]	15.29	0.69	14.16	14.19	14.13	57	01 03 43.8	-73 39 43
		2	6028.969		15.44	0.82	14.31	14.29	14.23			
1355	7.483	2	5997.939	15.08	14.64	0.38	13.97	14.12	14.06	55	00 39 29.9	-73 38 06
		2	6028.940		14.93	0.51	14.16	14.21	14.15			
1599	7.498	2	6029.005		15.24	0.54	14.40			61:	00 52 14.1	-73 17 32
1758	7.499	2	6006.163	15.08[a]	14.77	0.40	14.16	14.26	14.20	58	00 56 43.9	-73 10 35
1592	7.534	2	6006.125		15.10	0.68	14.16			55:	00 51 58.6	-73 12 14
2081	7.607	2	5994.026	14.80[a]	14.67	0.77	13.46	13.50	13.44	41	01 07 29.6	-72 52 29
1582	7.681	2	5994.172	14.83[a]	15.13	0.58	14.18	14.08	14.02	54	00 51 44.7	-72 28 48
1393	7.722	2	5998.206		15.51	0.66	14.38			62:	00 42 23.3	-73 37 20
1709	7.894	2	5998.166	15.10[a]	15.65	0.84	14.53	14.35	14.29	62	00 55 28.4	-73 44 51
1764	7.735	2	5997.995	15.28[a]	15.31	0.69	14.37	14.36	14.30	62	00 56 47.9	-72 36 10
845	7.950	2	5994.115	14.85[a]	15.07	0.62	14.10	14.03	13.97	54	00 58 11.3	-73 08 00
1396	8.061	3	5990.038	14.93[a]	15.51	0.70	14.40	14.21	14.15	59	00 42 46.3	-73 24 37
1632	8.126	2	5993.122	15.16[a]	15.23	0.58	14.28	14.26	14.20	60	00 53 19.3	-72 31 05
1415	8.141	2	5993.159		15.65	0.78	14.45			66:	00 44 09.2	-73 39 32
1589	8.332	2	5998.051		15.68	0.92	14.43			66:	00 51 55.7	-73 10 52
1437	8.376	2	5993.085	15.51	15.24	0.76	13.92	14.01	13.95	55	00 46 06.7	-73 12 50
1338	8.493	3	5990.126	15.20[a]	14.82	0.35	14.20	14.33	14.27	64	00 36 20.8	-74 05 22
1784	8.682	2	5997.962	15.18[a]	15.04	0.55	14.13	14.18	14.12	60	00 57 32.8	-73 18 10
1411	8.849	2	5992.958		14.11	0.54	13.75			50:	00 43 53.8	-73 40 18
1790	8.872	3	5990.203	14.98[a]	14.84	0.44	14.09	14.14	14.08	60	00 57 39.9	-73 07 30
2103	8.984	2	5993.934	15.16	15.91	0.70	14.50	14.25	14.19	64	01 08 44.0	-73 26 34
2087	9.159	2	5993.986	15.26	15.04	0.58	14.11	14.18	14.12	62	01 07 33.6	-72 36 03
836	9.403	2	5993.960	14.82	14.52	0.45	13.78	13.88	13.82	55	00 54 07.8	-71 48 27
1334	9.451	2	5992.131	14.92[a]	15.33	0.82	14.20	14.06	14.00	60	00 34 19.8	-74 02 57
1487	9.560	2	5993.237	14.83[a]	15.42	0.86	14.25	14.05	13.99	60	00 48 17.4	-72 59 25
1768	9.808	1	5943.147		15.34	0.81	14.06			61:	00 56 52.9	-72 25 16
6320	10.093	3	5990.027	14.88[a]	15.25	0.80	14.10	13.98	13.92	60	00 08 00.4	-75 27 19
2060	10.184	1	5914.204	14.34[a]	14.48	0.57	13.57	13.52	13.46	49	01 06 24.5	-72 32 54
818	10.335	1	5900.137	14.78[a]	14.74	0.49	13.99	14.03	13.97	62	00 38 29.3	-73 56 52
1426	10.438	2	5992.983		15.02	0.61	13.92			60:	0C 44 48.8	-73 15 41
1705	10.758	3	5990.190	15.08[a]	15.09	0.72	14.09	14.09	14.03	66	00 55 11.9	-73 08 24
1382	10.883	2	5993.009		14.89	0.61	13.80			58:	00 41 55.4	-73 30 51
2063	11.166	3	5990.215	14.78	14.83	0.70	13.81	13.79	13.73	58	01 06 09.5	-72 03 28
1471	11.192	2	5993.204		15.36	0.91	14.09			67:	00 47 37.4	-73 10 01
1630	11.401	2	5992.037	15.02	14.83	0.60	14.01	14.07	14.01	67	00 53 16.2	-73 20 10
2017	11.407	1	5943.255	14.74	14.26	0.44	13.47	13.63	13.57	55	01 04 42.2	-72 09 33
1610	11.644	3	5990.228	14.71	14.70	0.59	13.78	13.78	13.72	60	00 52 44.5	-72 40 54
857	11.982	3	5990.074	14.49	14.70	0.74	13.62	13.55	13.49	54	01 06 18.1	-74 00 31
1682	12.149	3	5990.165	14.73	15.04	0.83	13.87	13.77	13.71	61	00 54 41.3	-73 39 28
1365	12.413	3	5990.101	15.03	14.94	0.61	13.97	14.00	13.94	68	00 39 56.2	-74 00 09
2227	12.466	3	5990.062	14.82	14.51	0.59	13.61	13.71	13.65	60	01 25 05.6	-74 23 39
2230	12.526	3	5990.049	14.69	14.36	0.64	13.41	13.52	13.46	55	01 26 54.7	-73 04 24
2052	12.574	1	5942.293	14.30	14.14	0.46	13.30	13.35	13.29	51	01 06 37.6	-73 19 26

TABLE 1—*Continued*

HV. (1)	P. (days) (2)	Tel. (3)	J. D. 2440000+ (4)	<V> (5)	V (6)	(B−V) (7)	I_V (8)	$\langle I_V \rangle$ (9)	$\langle I_V \rangle_o$ (10)	Dist. (Kpc) (11)	R. A. (1950) h. m. s. (12)	Dec. (1950) ° ′ ″ (13)
1744	12.623	1	5902.165	14.59	14.76	0.81	13.64	13.58	13.52	57	00 56 02.9	−72 32 37
1873	12.941	3	5990.145	14.91	14.67	0.77	13.60	13.68	13.62	60	01 00 09.4	−72 45 17
1351	13.084	1	5914.141	14.68[a]	14.74	0.60	13.88	13.86	13.80	66	00 39 09.8	−73 48 06
2225	13.154	1	5970.200	14.80	14.70	0.92	13.43	13.46	13.40	55	01 23 16.9	−74 32 28
2202	13.182	1	5943.174	14.44	14.40	0.79	13.23	13.24	13.18	50	01 13 54.2	−72 57 34
1464	13.295	2	5992.938		15.32	1.05	13.84			66:	00 47 14.5	−73 29 05
2189	13.459	1	5970.249	14.53	14.90	0.79	13.76	13.64	13.38	61	01 12 00.6	−72 44 15
827	13.465	1	5609.172	14.53	14.60		13.75	13.73	13.67	63	00 47 54.4	−72 46 05
1345	13.476	3	5990.017	14.58[a]	14.58	0.74	13.50	13.50	13.44	57	00 38 43.3	−73 29 41
1438	13.646	2	5991.988	15.47	15.06	0.91	13.66	13.80	13.74	66	00 46 07.0	−73 18 22
1373	13.709	3	5990.090	14.90[a]	14.52	0.58	13.61	13.74	13.68	64	00 41 36.7	−73 16 34
1326	13.727	3	5990.006	14.91	15.31	0.99	13.98	13.85	13.79	68	00 31 20.9	−73 39 38
1933	13.781	1	5942.224	14.28	14.57	0.58	13.64	13.54	13.58	59	01 01 42.0	−72 16 22
10366	14.135	1	5969.975		14.43	0.65	13.38			55:	01 03 27.0	−74 28 33
1996	14.240	1	5969.222	15.03[a]	15.11	0.90	13.91	13.88	13.82	70	01 04 20.9	−73 06 44
1335	14.380	1	5970.097	14.80	14.72	0.75	13.61	13.64	13.58	63	00 34 58.3	−74 13 00
1386	14.428	1	5970.151	14.80	15.74	0.55	14.76	14.45	14.39	88	00 41 55.5	−73 36 32
		2	6030.103		15.42	0.53	14.49	14.28	14.22			
1579	14.573	1	5970.058	14.46	14.83	0.61	13.70	13.58	13.52	62	00 51 34.8	−73 23 12
2088	14.578	3	5989.997	14.70	14.94	0.79	13.86	13.78	13.72	68	01 06 53.1	−71 40 55
1695	14.596	1	5970.024	14.73	14.99	0.76	13.73	13.64	13.58	64	00 54 55.0	−72 33 23
843	14.714	1	5969.935	15.05	14.78	0.82	13.57	13.66	13.60	64	00 56 50.4	−72 43 13
2233	15.172	1	5967.226	13.97	13.96	0.68	12.87	12.87	12.81	46	01 34 52.9	−74 08 40
1442	15.287	1	5968.253	14.85	14.41	0.59	13.42	13.57	13.51	63	00 46 07.3	−73 34 58
1560	15.509	1	5968.154	14.83	14.59	0.82	13.51	13.59	13.53	64	00 50 49.9	−73 14 30
12108	15.610	1	5943.082		14.01	0.48	13.14			53:	00 52 09.1	−72 43 24
1481	15.651	2	5994.262		14.70	1.16	12.97			49:	00 47 54.5	−73 30 26
1372	15.774	1	5968.180	14.94[a]	15.47	1.20	13.86	13.68	13.62	68	00 41 19.8	−73 35 57
1482	15.827	1	5968.218	14.92	15.76	1.50	13.68	13.40	13.34	60	00 47 58.1	−73 24 43
1328	15.840	1	5966.078	14.14	13.75	0.42	13.01	13.14	13.08	53	00 30 53.2	−74 05 52
854	15.953	1	5942.151	14.30	13.82	0.35	13.20	13.36	13.30	59	01 05 15.5	−73 32 25
1787	16.196	1	5902.174	14.29	13.97	0.70	12.93	13.04	12.98	51	00 57 24.1	−72 19 56
11210	16.218	1	5966.155	14.43	14.63	1.07	13.26	13.19	13.13	55	02 02 26.1	−74 17 48
1333	16.289	1	5968.074		14.91	0.96	13.66			68:	00 34 05.1	−74 12 31
828	16.296	1	5968.045		14.84	0.70	13.69			69:	00 48 08.3	−73 29 42
1533	16.435	1	5968.125		15.12	1.14	13.82			74:	00 49 54.2	−73 17 48
1954	16.700	1	5914.246	13.87	14.16	0.72	12.97	12.87	12.81	50	01 02 24.2	−72 30 06
		1	5943.288		14.10	0.77	13.01	12.93	12.87			
		1	5968.000		13.82	0.56	12.91	12.93	12.87			
822	16.742	1	5900.155	14.57	14.32	0.83	13.22	13.30	13.24	59	00 40 02.5	−73 48 51
1925	17.199	1	5938.214	14.00	13.98	0.67	12.97	12.98	12.92	52	01 01 41.4	−72 49 10
1478	17.532	1	5967.960		15.43	1.09	13.95			82:	00 47 44.0	−73 35 26
10386	17.741	1	5967.187	14.26	14.59	0.96	13.25	13.14	13.08	57	01 47 24.9	−73 18 25
1342	17.938	1	5914.112	14.22	14.27	0.63	13.39	13.37	13.31	63	00 37 38.7	−74 01 22
1884	18.116	1	5943.107	14.46	14.26	0.91	13.09	13.16	13.10	58	01 00 19.5	−72 27 58
817	18.892	1	5969.148	13.90	13.77	0.67	12.74	12.78	12.72	50	00 37 17.3	−72 18 27
1541	19.326	1	5938.186		14.41	0.86	13.24			62:	00 50 04.1	−73 25 39
1543	20.454	1	5966.181	14.85	14.50	0.95	13.23	13.35	13.29	68	00 50 05.0	−73 38 13
11211	21.379	1	5966.116	13.87	13.89	0.99	12.58	12.58	12.52	49	02 20 22.9	−73 18 49
1522	22.143	1	5942.094	14.40	14.56	1.23	13.00	12.95	12.89	59	00 49 26.6	−73 27 48
2209	22.650	1	5967.161	13.57	13.19	0.44	12.37	12.49	12.43	48	01 16 34.8	−73 53 13
1430	23.972	1	5942.054	14.34[a]	14.58	1.09	13.10	13.02	12.96	64	00 45 20.9	−73 14 00
11129	24.475	1	5943.036	14.53[a]	15.15	1.21	13.51	13.30	13.24	73	00 46 17.4	−73 08 47
2205	25.432	1	5967.141	14.11	14.40	1.14	12.92	12.82	12.76	60	01 15 39.6	−73 58 59
847	27.057	1	5914.178	13.96	13.53	0.60	12.60	12.74	12.68	60	00 59 23.6	−72 28 03
1501	27.406	1	5966.270	14.06	14.43	1.00	12.97	12.85	12.79	64	00 48 52.2	−73 13 53
819	28.443	1	5938.042	14.09	13.65	0.57	12.77	12.92	12.86	67	00 38 52.0	−73 59 35
MKd	28.6	1	5942.024		14.59	0.70	13.40			78:	00 48 06.6	−73 31 01
		2	6029.959		14.59	1.20	13.07					
1967	28.935	1	5914.239	13.67	14.04	0.93	12.72	12.60	12.54	59	01 02 47.8	−72 16 40
863	28.961	1	5966.097	13.40	13.59	1.00	12.26	12.20	12.14	49	01 27 24.3	−74 03 19
12951	29.989	1	5942.273		14.05	1.03	12.58			60:	01 06 43.6	−72 46 11
		1	5967.114		13.93	0.97	12.63					
1451	30.063	1	5938.108	14.05	14.41	1.14	12.97	12.85	12.79	64	00 46 36.5	−73 29 53
		1	5942.997		13.57	0.73	12.52	12.68	12.62			
823	31.925	1	5609.116	13.81	13.46		12.32	12.44	12.38	58	00 41 57.4	−73 53 15
10357	32.012	1	5967.065	14.02	14.30	1.02	12.77	12.68	12.62	64	00 48 34.3	−73 23 49
1636	32.746	1	5966.212	13.84	14.59	0.65	12.39	12.14	12.08	51	00 53 19.9	−73 02 19
855	32.941	1	5942.177	13.77[a]	13.50	0.80	12.36	12.45	12.49	59	01 05 47.7	−73 29 27
840	33.039	1	5902.139	13.64	13.70	1.10	12.28	12.25	12.19	54	00 56 12.1	−72 40 56
865	33.326	1	5966.052	13.17	12.85	0.64	11.84	11.95	11.89	47	01 39 40.9	−74 45 36
2064	33.663	1	5938.256	13.77	13.42	0.72	12.31	12.43	12.37	59	01 06 40.0	−72 47 18
2231	36.679	1	5967.028	13.56	13.84	1.16	12.33	12.24	12.18	57	01 29 17.3	−73 34 09
MKg	38.7	3	5967.005	13.54	13.42	0.79	12.20	12.24	12.18	59	00 49 40.2	−73 09 37
11182	39.199	1	5943.227	13.72	13.37	0.79	12.30	12.42	12.36	64	00 55 51.2	−72 20 26
LV52	41.405	1	5966.247		13.60	0.95	12.24			61:	00 50 15.8	−73 21 40
2195	41.783	1	5620.991	13.04	12.90		11.67	11.72	11.66	49	01 13 02.6	−72 55 44
		3	5684.164		13.36		11.89	11.78	11.72			
837	42.680	1	5621.037	13.27	13.21		11.80	11.82	11.76	50	00 54 11.6	−72 15 18
		3	5684.158		13.13		11.65	11.70	11.64			
1877	49.667	1	5938.218	13.20	12.87	0.74	11.79	11.90	11.84	58	01 00 10.6	−72 21 53
		1	5942.257		12.85	0.82	11.74	11.86	11.80			
824	65.798	1	5609.147	12.41	12.05		11.05	11.15	11.09	48	00 45 02.6	−72 59 13
		1	5621.065		12.21		11.08	11.13	11.07			
		1	5968.276		12.56	1.11	11.19	11.14	11.08			
11157	68.908	1	5914.160	12.95	12.84	0.92	11.56	11.60	11.54	61	00 51 09.5	−72 11 20
		1	5943.205		12.99	1.11	11.57	11.56	11.50			
834	73.589	1	5938.073	12.22	12.53	1.09	11.14	11.04	10.98	49	00 51 57.1	−72 33 30
829	87.627	1	5609.211	11.94	11.76		10.62	10.68	10.62	46	00 48 41.8	−73 01 28
		1	5621.076		11.94		10.69	10.69	10.63			
821	127.78	1	5914.096	11.96	11.65	0.90	10.48	10.58	10.52	55	00 39 50.4	−73 59 51
		1	5967.922		12.18	1.31	10.58	10.51	10.45			

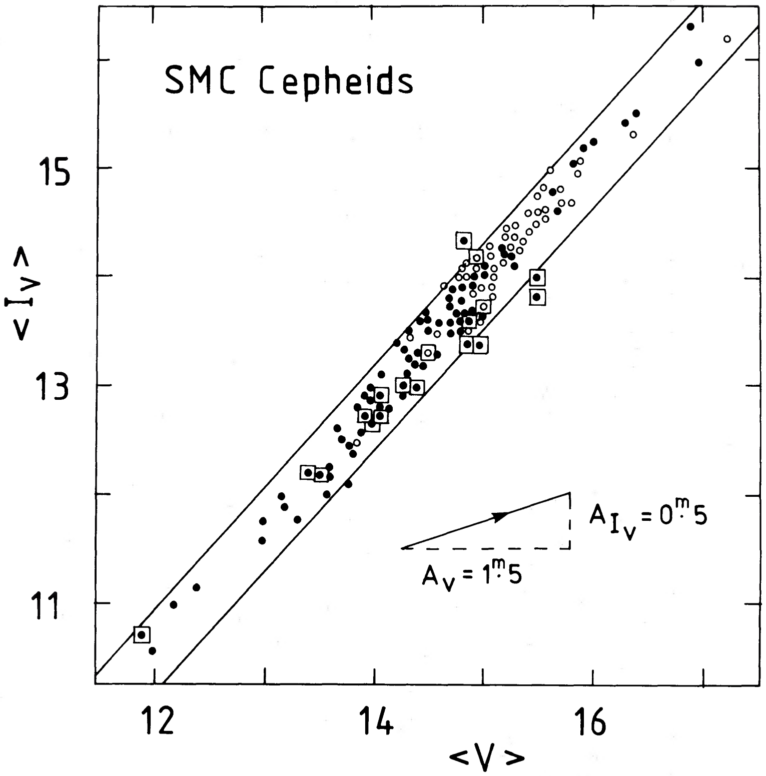

FIG. 2.—$\langle I_V \rangle$, the mean near-infrared (1.05 μm) magnitudes, plotted against $\langle V \rangle$, the mean visual magnitudes for the SMC Cepheids. The filled and open circles denote the photoelectric and photographic values of $\langle V \rangle$ respectively. The points in boxes are for Cepheids in the central region of the Bar. The reddening line is shown at the bottom of the diagram.

The relative distances for those corrected to mean light are accurate to about $\pm 4\%$, i.e., to about ± 3 kpc at the distance of the SMC. The random phase relative values (denoted by colons) are accurate to about $\pm 6\%$, i.e., to about ± 4 kpc.

Columns (*12*) *and* (*13*).—The right ascension and declination (1950.0) for each Cepheid accurate to $\pm 2''$.

d) *Interstellar Reddening*

Caldwell and Coulson (1985) have thoroughly investigated the use of *BVI* colors to derive accurate individual reddenings of Cepheids. A mean E_{B-V} is found for the SMC of $0^m.054$ with a dispersion of 0.021. No large-scale gradient or segregation of the values is noticeable, although no Cepheids were observed in the central region of the Bar. A uniform correction for reddening for all Cepheids of $A_{I_V} = 0^m.06$ is applied to all the I_V measurements. The ratio $R = A_V/E_{B-V}$ is taken as 3 in the SMC (Feast and Whitelock 1984), and the extinction in the I_V waveband is taken as one-third that in the V band.

Justification for using a uniform reddening correction for the SMC (including the Bar region) is given by the plot in Figure 2 of $\langle I_V \rangle$ against $\langle V \rangle$. The points in boxes are for the Cepheids in the central region of the Bar. These show no sign of reddening different from that for any other region in the SMC.

III. THE P-L RELATION

The P-L relations in $\langle I_V \rangle_0$ for the SMC and LMC are plotted in Figure 3. The values for the LMC are from Visvanathan (1985), plus an additional 13 which were measured during the SMC observations. The least-squares solution for the LMC is

$$\langle I_V \rangle_0 = 16.36 - (2.90 \pm 0.07) \log P , \quad \sigma = 0^m.13 .$$

The Cepheids on the eastern side of the LMC show distance moduli systematically lower by $0^m.1$ than those on the western side. This systematic difference is due to the 30° tilt of the plane of the LMC to the plane of the sky (Gascoigne and Shobbrook 1978; Martin, Warren, and Feast 1979; Caldwell and Coulson 1986). Therefore the dispersion of $0^m.13$ found in the P-L relation is mainly due to the geometry of the LMC. Hence the error in the ratio of our distance measurements of SMC Cepheids depends primarily on the accuracy of measurement of the difference in magnitudes of the individual Cepheids (i.e., $0^m.04$).

In the past year, more multiphase observations of $\langle I_V \rangle$ have been obtained for 16 Cepheids which are members of open clusters and associations in our Galaxy. These data have been combined with those given by Visvanathan (1985) to form a new base for the analysis of the P-L relation in I_V. The absolute magnitude $M_{\langle I_V \rangle_0}$ for each Cepheid has been computed from the distance moduli given by Caldwell (1983). These values are preferred to those used by Visvanathan (1985) as they take into account metallicity variations from cluster to cluster. RS Pup, V810 Cen, and TW Nor were omitted from the analysis for the reasons given in Caldwell (1983). Adopting the slope of the P-L relation in the LMC, the new absolute calibration is

$$M_{\langle I_V \rangle_0} = -2.06 \pm 0.04 - (2.90 \pm 0.03) \log P ; \quad \sigma = 0^m.18 .$$

The distances given in Table 1 were calculated using this calibration and assuming the slopes of the P-L relations for the LMC and SMC are similar.

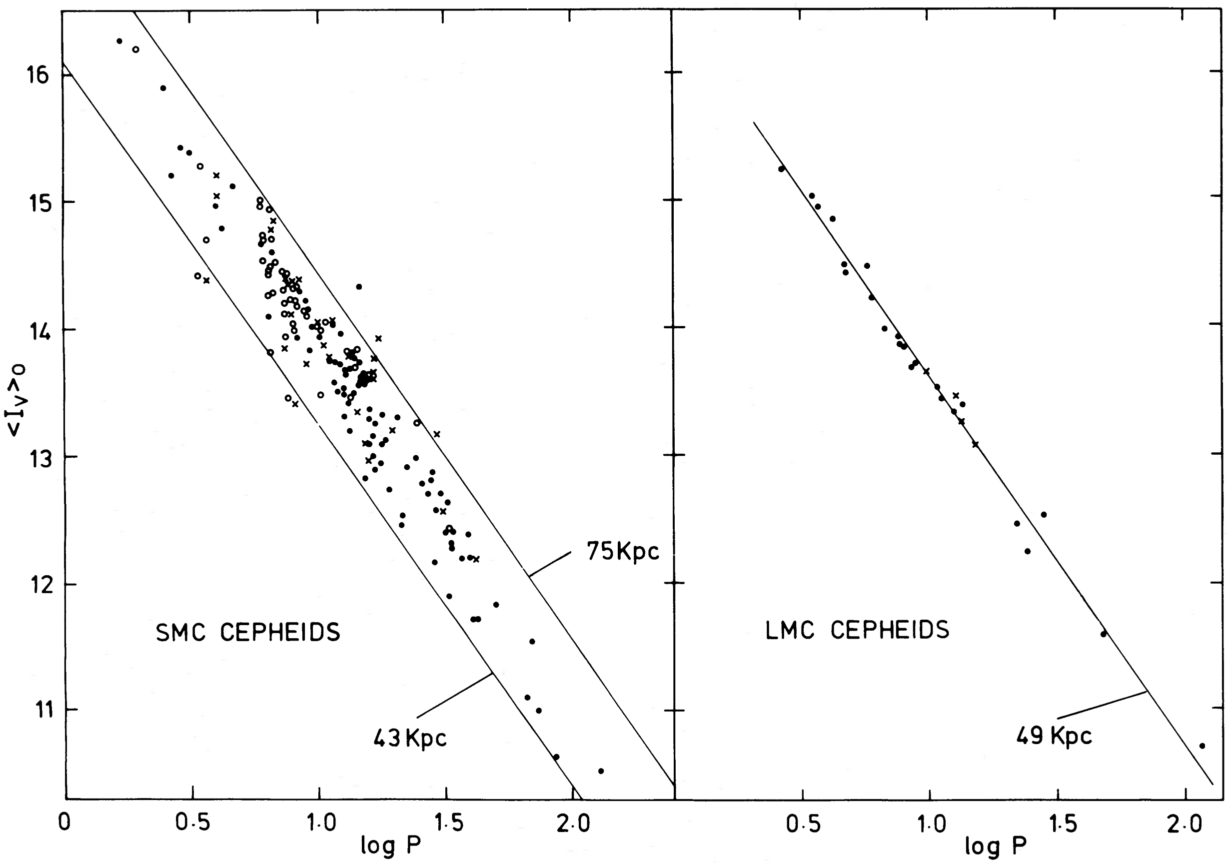

FIG. 3.—The period-luminosity relationship for the LMC and SMC. The line in the LMC represents the least-squares fit to the points. Using the absolute calibration described in text, it corresponds to a distance of 49 kpc. The two lines drawn in the SMC have the same slope as the LMC line and form approximately the outer envelope to the points. They correspond to distances of 43 and 75 kpc. The filled and open circles indicate Cepheids for which photoelectric and photographic values of $\langle V \rangle$ respectively have been used to derive $\langle I_V \rangle$. The crosses indicate Cepheids which have only random phase I_V measurements.

IV. DISCUSSION

a) *The Space Distribution of SMC Cepheids*

The classical Cepheid of period greater than 10 days (age $< 5 \times 10^7$ yr) has been used successfully by Kraft and Schmidt (1963) to trace the spiral structure of our Galaxy; and Payne-Gaposchkin and Gaposchkin (1966) found that the young Cepheids are distributed over the face of the SMC similarly to the OB stars, emission nebulae, and H I. Cepheids with periods less than 10 days have a much broader distribution both in our Galaxy and the SMC. Therefore the younger Cepheids should outline more accurately the distribution in depth of the gas in the SMC.

The histograms in Figure 4 show the distribution of distances of Cepheids in the main body of the SMC for periods greater than and less than 10 days. The sample is 85% complete for Cepheids of period greater than 10 days but much less complete for shorter periods. Therefore the different distributions between the short- and long-period Cepheids displayed in Figure 4 are not significant. Therefore any discussion of the relative distributions of the short- and long-period Cepheids must wait until more complete samples of the short-period Cepheids are obtained. The histograms in Figure 5 indicate the distribution of the distances of the Cepheids in each of the subsystems defined in Figure 1. The shading differentiates between the short- and long-period Cepheids.

In Figure 6*b*, the distance of each Cepheid in the main body of the SMC is plotted against its projected position onto the major axis; and in Figure 6*a*, the distance of each Cepheid in the Bridge is plotted against its projected position onto the H I ridge line of the Bridge. The (x, y)-scales are about equal in these plots. The angular distances along the major axis and ridge line have been converted to linear dimensions by assuming a mean distance to the SMC of 60 kpc. Both major axis and ridge line are drawn on Figure 1. Figure 7 is a similar plot for Cepheids in the main body of the SMC but with the distance scale of the Cepheids greatly compressed to facilitate the identification of structure in their distribution. The distance scale of the Cepheids is 1/20 the scale for distance along the major axis.

These plots reveal the great depth of the SMC shown by these Cepheid distance measurements. Omitting the extreme values, the Cepheids extend from 43 to 75 kpc, with a maximum concentration at 59 kpc. The depth of 32 kpc is much greater than the 5 kpc anticipated on the basis of their areal distribution. It is in qualitative agreement with the range of distance moduli of blue supergiant stars measured by Ardeberg and Maurice (1979); Azzopardi (1981); Florsch, Marcout, and Fleck (1981); and Tully and Wolff (1984). It is also in agreement with the recent *BVR* observations of 63 Cepheids in the SMC by Caldwell and Coulson (1986). Their Cepheids show a depth of 22 kpc, ranging in distance from 53 to 75 kpc.

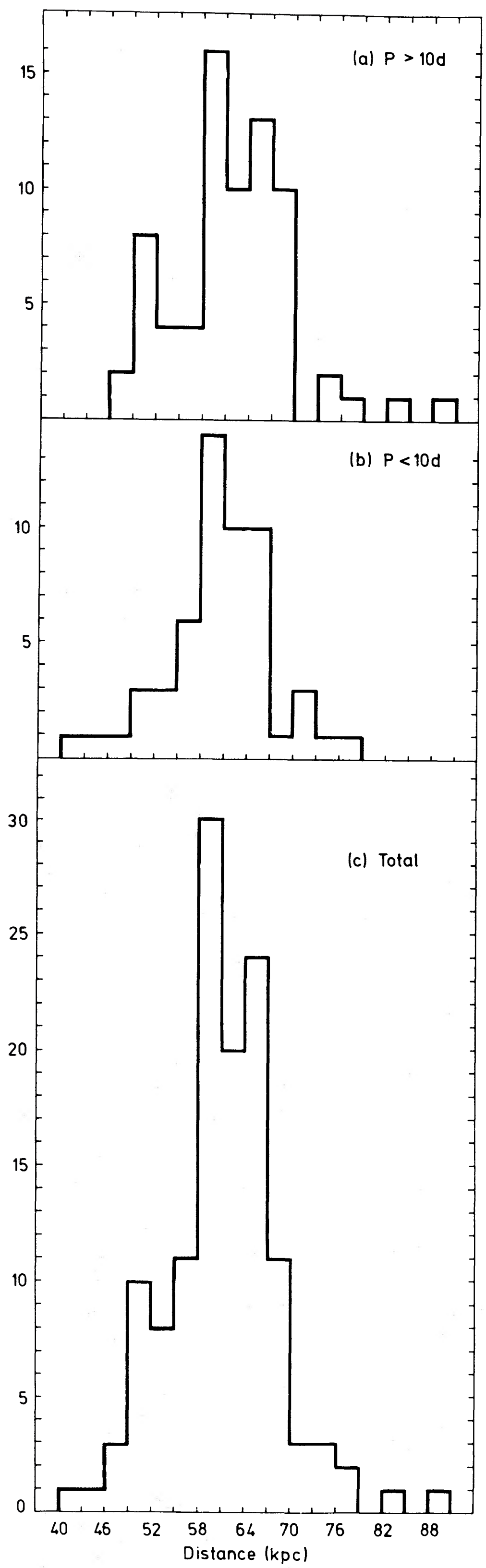

FIG. 4.—The distribution of distances of the observed Cepheids in the main body of the SMC (Bar, southwest region, and northern arms in Fig. 1); (*a*) and (*b*) are for Cepheids with periods greater than and less than 10 days respectively; (*c*) is for all the Cepheids in the main body.

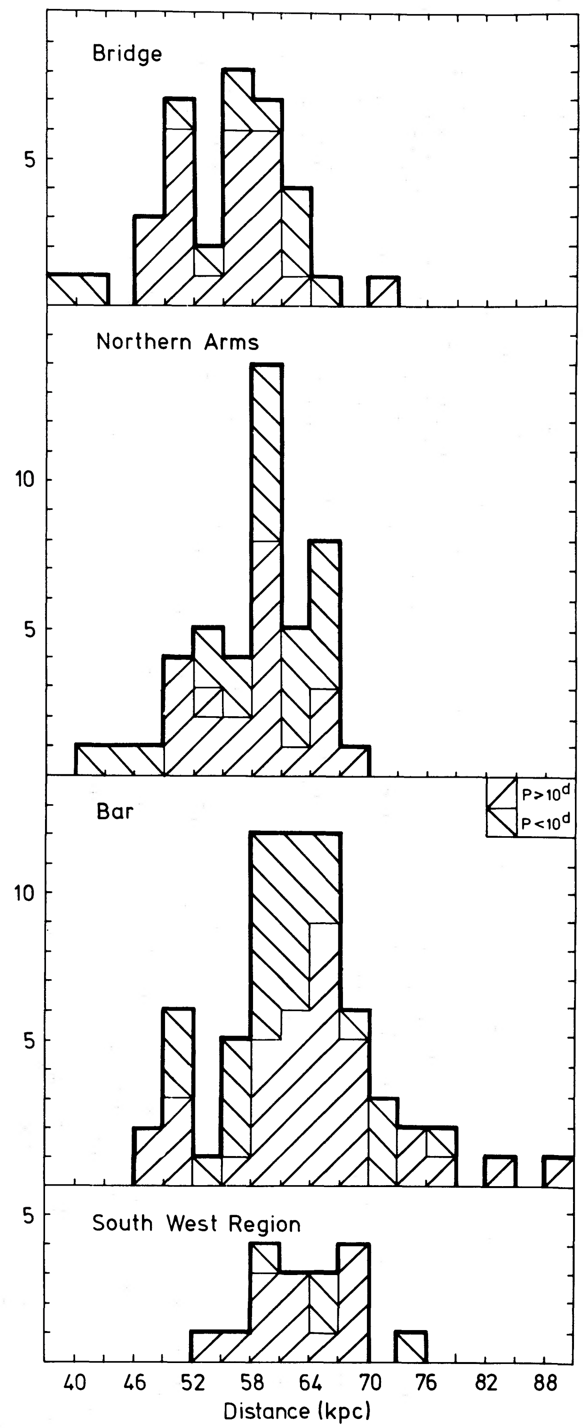

FIG. 5.—The distribution of distances of the SMC Cepheids within the four subsystems defined in Fig. 1. The shading differentiates between the Cepheids with periods greater than and less than 10 days respectively.

b) The Interstellar Absorption Lines of Ca II

The problem is to tie in the geometry of the SMC as revealed by these Cepheid observations with the radial velocity measurements of the H I, OB stars, and emission nebulae. In velocity-space, there are two clearly identifiable systems, one with a radial velocity lower than the other by about 40 km s^{-1} (Mathewson 1984). A good clue that they are spatially separat-

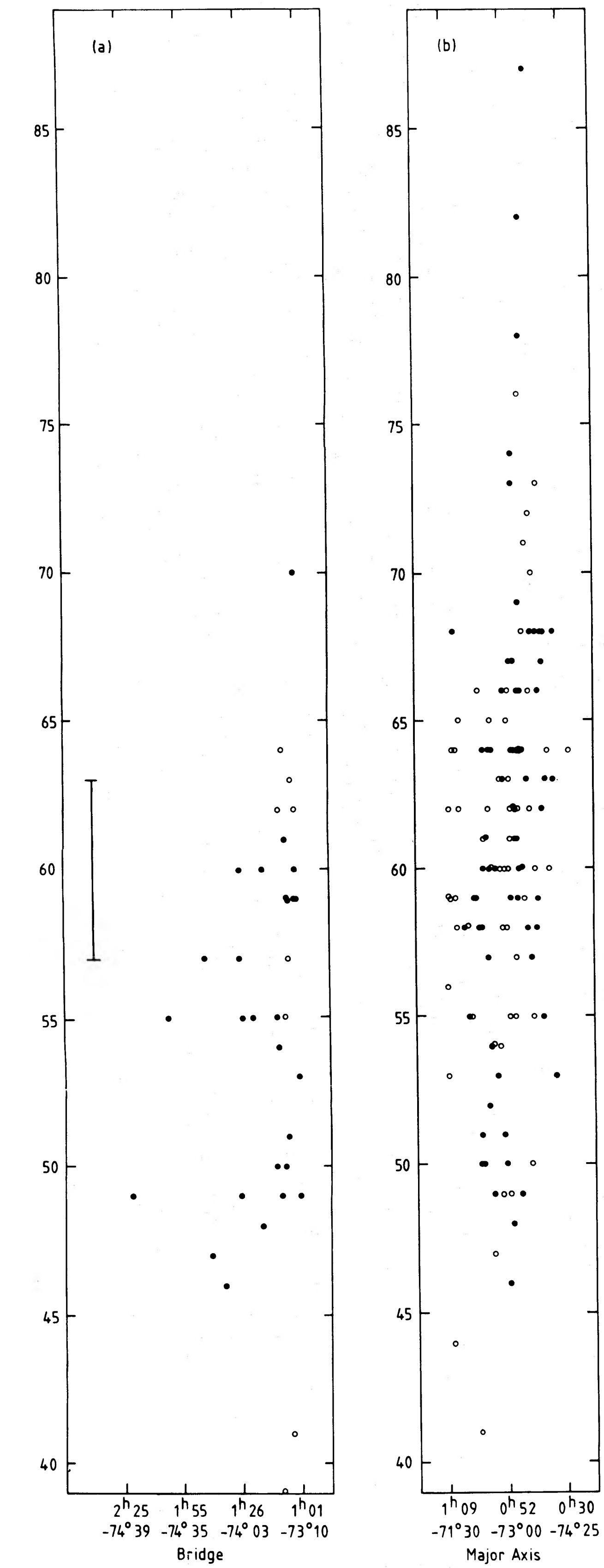

FIG. 6.—(*a*) The distances of the SMC Cepheids lying within the Bridge subsystem (Fig. 1) are plotted against their projected positions onto the ridge line of the Bridge. (*b*) The distances of the Cepheids in the main body of the SMC are plotted against their projected positions onto the major axis (Fig. 1). The *x* and *y* scales of distance are approximately the same. The angular distances along the major axis and ridge line have been converted to linear dimensions by assuming a mean distance to the SMC of 60 kpc. The filled and open circles denote Cepheids with periods greater than and less than 10 days. The vertical bar in (*a*) represents the error bar for the distance measurement of each Cepheid, i.e., ± 3 kpc.

ed is given by the interstellar Ca II absorption lines observed in the spectra of some SMC stars. Figure 8 presents data by Feast, Thackeray, and Wesselink (1960); Thackeray (1978); Cohen (1984); and Mathewson and Ford (1985) of the radial velocities of SMC stars and their associated interstellar Ca II absorption lines. The H I profile at the position of each star is given. These data give a fair coverage of the SMC, and it is seen that without exception, the absorption line is at a lower velocity than the star. In 13 of the cases, the star is associated with the high-velocity component of H I while the absorption line is produced by the low-velocity component. This is compelling evidence that the low-velocity component is in front of the high-velocity component and that the two systems are separating at 40 km s^{-1}. In the other cases, the absorption line is produced in the same component as the star but at a lower velocity. This suggests that the broadening of the H I line is not produced by random turbulence but by a systematic expansion of both low- and high-velocity components. The average half-widths of the peaks in the H I profiles are about 30 km s^{-1}, so each system may itself be expanding at 15 km s^{-1}.

c) *The Geometry of the SMC*

Figure 7 is useful in attempting to identify the high- and low-velocity components in the main body of the SMC. The solid lines envelop the young Cepheids (*filled circles*), and the dashed lines demarcate what is considered to be the low-velocity (near) and high-velocity (far) components. The bright central zone of the Bar around 00^h50^m, $-73°15'$ is the most extended (45–90 kpc), and this is reflected in the complexity of the H I profiles in this direction (see Fig. 4 of Mathewson and Ford 1984). The low-velocity component is separated into two groups, one at 50 kpc (center to northeast) and the other at 60 kpc (Bar to southwest); they form part of the overall gradient in distance from southwest to northeast of the SMC also observed by Florsch, Marcout, and Fleck (1981); Welch and Madore (1984); and Caldwell and Coulson (1985*b*).

The histogram for the Bridge in Figure 5 shows a bifurcation of young Cepheids with peaks at 50 and 58 kpc which are identified with the low- and high-velocity components respectively, seen in the H I. These distances indicate that the Bridge is bifurcated and on average closer than the median distance of the SMC (~ 60 kpc) and will join with the LMC, which is at a distance of 50 kpc.

The best way to match the structural and kinematical features of the Population I component of the SMC is to measure the systemic radial velocities of the young Cepheids in Table 1. Unfortunately, this measurement is difficult because Cepheids vary in radial velocity by about 60 km s^{-1} during each period (Sanford 1956). However, Wallerstein (1984) has measured the systemic velocity of five Cepheids in the main body of the SMC listed in Table 1 by assuming that they have velocity curves of the same shape and amplitude as the 43 day Cepheid SV Vul.

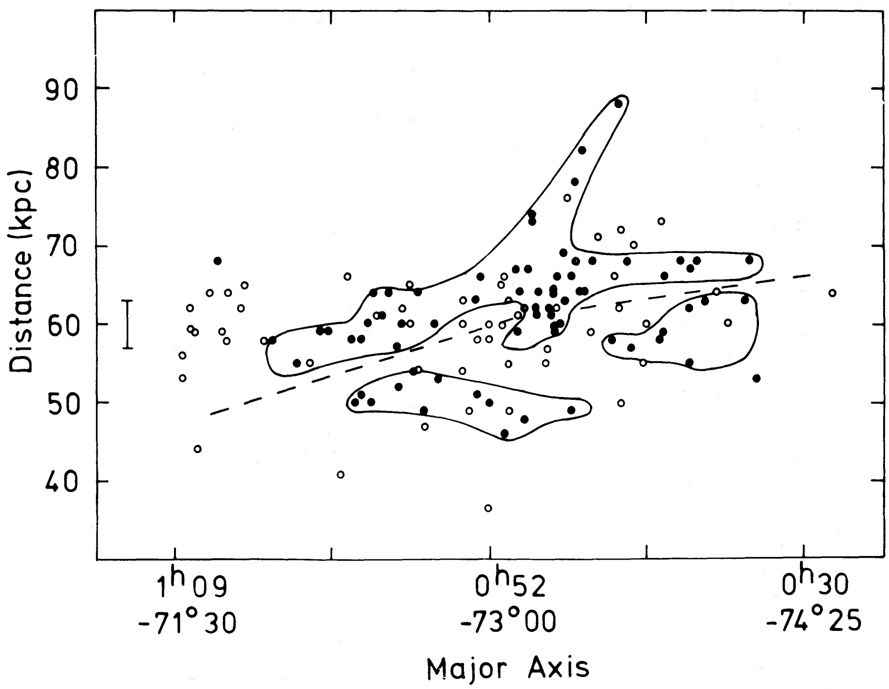

FIG. 7.—This plots the same data as in Fig. 6*b*, i.e., the distances of the Cepheids in the main body of the SMC against their projected positions onto the major axis. However, the *y*-scale for the distances of the Cepheids is compressed by a factor of 20 with respect to the *x*-scale for the distance along the major axis. This facilitates identification of structure in the depth distribution of the Cepheids. The filled and open circles denote the Cepheids with periods greater than and less than 10 days. The solid lines envelop the longer period Cepheids. The dashed lines demarcate between the near and far groups of Cepheids. The error bar for the distance measurement of each Cepheid is shown at the left of the figure.

Unfortunately, his published data are in error, but Figure 9 plots the corrected values (Wallerstein 1985). Also plotted are measurements of HV 1338 and HV 1365 (Caldwell and Coulson 1986). Five of the seven agree approximately with the separation defined in Figure 7. However, the numbers are small, and the measurement of many more radial velocities is the next step in this program.

d) The "Tidal" Model of Murai and Fujimoto (1980)

The results of these Cepheid distance measurements are in good agreement with that predicted by the "tidal" model generated by Murai and Fujimoto (1980) to explain the Magellanic Stream. They found that the tidal interaction between the LMC and SMC would form a bridge between the two galaxies and a short tail on the SMC. Under the influence of the gravitational force of our Galaxy, this short tail kinematically evolves into a much longer tail which models quite well with the Magellanic Stream. An important consequence of their computer simulations is that the SMC had a collision with the LMC some 2×10^8 yr ago.

Figure 7 of Murai and Fujimoto (1980) shows the radial distance of the SMC test particles at the present time as a function of Magellanic longitude, i.e., angular distance along the Magellanic Stream. In the direction of the SMC, the test particles are distributed from 50 to 80 kpc, matching the distribution of distances of the Cepheids in Figure 6. No clear bifurcation is seen in the distribution of the test particles. However, it should be remembered that in the collision, the stars would have behaved like the test particles in the computer simulations, but the gas would have been affected by gas-gas collisions. The observed Cepheids, whose ages range from 10^7 yr to 1–2 $\times 10^8$ yr, were all born after the collision, so they should follow the gas kinematics. Therefore there may be some difference between the computer simulations and the observed distribution of gas and Cepheids.

The radial velocities of the test particles are given in Figure 8*b* of Murai and Fujimoto (1980), which show a range of 140 km s^{-1} with two peaks separated by 60 km s^{-1}, in fair agreement with that observed. Along the line of sight through the SMC, the higher the radial velocity, the more distant the test particle, in accord with the absorption line observations.

Mathewson and Ford (1984) have suggested that the collision tore the SMC in half, and for 2×10^8 years the fragments have been separating at 40 km s^{-1}. The nearer fragment at the lower radial velocity is called the Small Magellanic Cloud Remnant (SMCR), and the more distant fragment at the higher radial velocity is called the Mini-Magellanic Cloud (MMC). It is suggested above that each fragment itself is expanding at about 15 km s^{-1}, so that the SMCR and MMC should have a depth of at least 6 kpc with their centers 8 kpc apart, i.e., a total extent of 14 kpc. In Figure 7, the two components outside the central zone are on average about 10 kpc apart with an overall depth of 17 kpc. The central zone is much deeper, extending from 45 to 90 kpc. Hence it appears that the SMC is more disrupted than predicted on the basis of the H I data.

Indeed, if the mass of the SMC is about $10^9\ M_\odot$, the mass of the Galaxy $7 \times 10^{11}\ M_\odot$, and the perigalactic distance of the SMC 60 kpc (Murai and Fujimoto 1980), then the tidal radius of the SMC is only 4 kpc. Hence the close encounter with the LMC plus the recent perigalactic passage of the SMC is stripping the SMC of much of its mass. The SMC is in the process of irreversible disintegration.

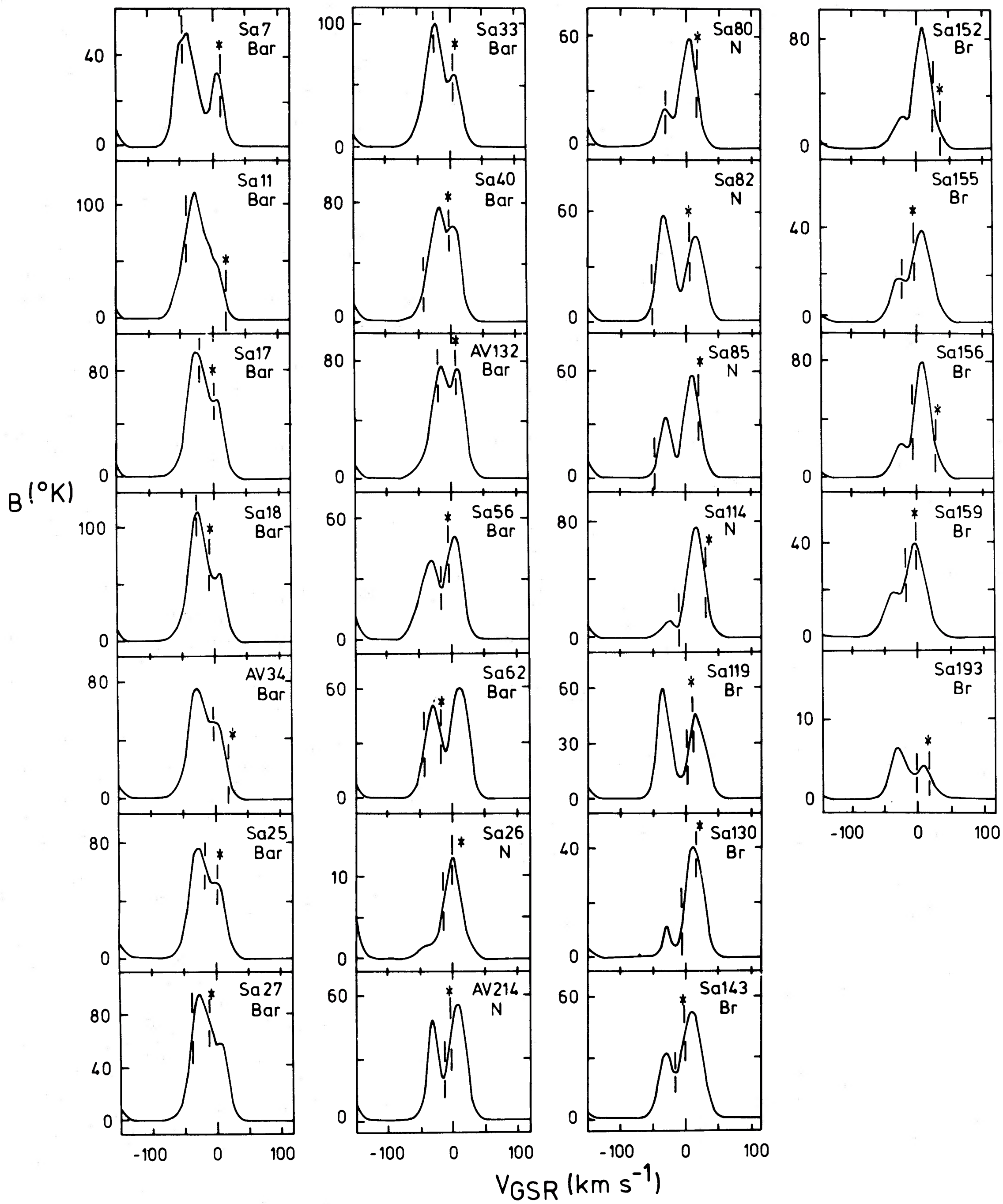

FIG. 8.—The radial velocities of 26 stars in the SMC and the interstellar Ca II absorption lines in their spectra have been marked on the H I profiles observed at the position of each star. The lines with asterisks indicate the stellar radial velocities, while the unmarked lines indicate the radial velocities of the absorption lines. In the top right-hand corner is the star number, taken from the catalogs of Sanduleak (1968) and Azzopardi and Vigneau (1975). The radial velocities have been corrected for a Galactic rotation of the Sun of 250 km s^{-1}. Underneath the star number, the subsystem in which the star lies is noted.

e) *The Model of Caldwell and Coulson* (*1986*)

Caldwell and Coulson (1986) interpret the H I velocity data and their Cepheid data for the SMC as indicating a central bar seen edge-on, a near arm (northeast), a far arm (southwest), and a mass of material pulled out of the center of the SMC and seen in projection in front of the far arm in the southwest. The far arm is associated with the lower velocity H I component, while the near arm and the material in front of the far arm is associated with the higher velocity H I component. This model does not adequately explain the observations, and our criticisms are:

1. The projected separation on the sky of the near and far arms is only 4 kpc, but their separation along the line of sight is 18 kpc (see Fig. 7 of Caldwell and Coulson 1986). With this geometry it is difficult to invoke normal galactic rotation to explain the difference in radial velocity of 70 km s^{-1} between the H I in the near and far arms.

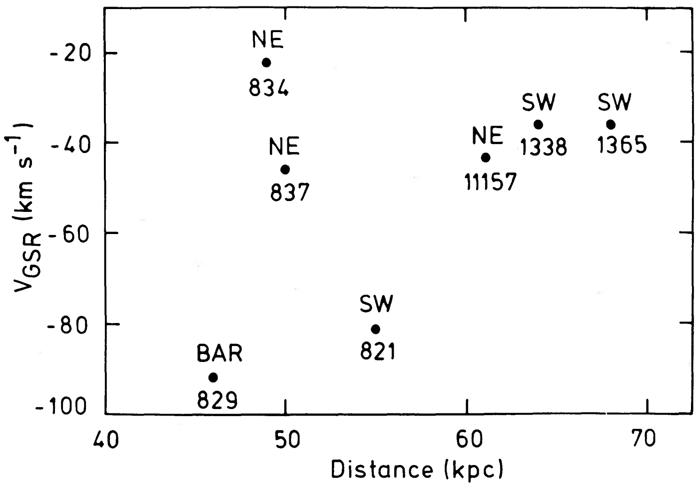

FIG. 9.—The radial velocities (corrected for a Galactic rotation of the Sun of 250 km s^{-1}) of seven Cepheids in the main body of the SMC measured by Wallerstein (1984, 1985) and Caldwell and Coulson (1986) are plotted against distances of the Cepheids. The HV number of each star and the subsystem in which it lies are marked.

2. The material which has been pulled out in front of the SMC from its center should have a lower radial velocity relative to the center. However, its observed radial velocity is higher than the center's.

3. The intense, low-velocity ridge centered on 00^h57^m, $-72°.7$ (see Fig. 4 of Mathewson and Ford 1984) is left out of their model.

4. In their Figure 14, a number of Cepheids which they plot as lying in the high-velocity H I at the northeast end of the major axis of the SMC really lie over 3° away in the Bridge. They have been projected onto the major axis from so great a distance that they cannot be associated with the H I shown in this figure.

5. Their model, which leads to an inverse correlation of velocity and distance, does not satisfy the results of the Ca II absorption line observations, which imply that the low-velocity component is in front of the high-velocity component. In general, tidal models show that as far as line-of-sight debris is concerned, the farthest material has the highest radial velocity while the closest has the lowest radial velocity.

The authors thank the 2.3 m telescope support staff for their help, particularly Dr. Gary Hovey and Mr. Hilton Lewis. They also wish to thank Dr. John Dawe, Officer-in-Charge of Siding Spring Observatory. We gratefully acknowledge the assistance of the AAT staff for their assistance during our observations with that telescope. We thank Dr. George Wallerstein for his private communication concerning his radial velocity measurements of Cepheids.

REFERENCES

Ardeberg, A., and Maurice, E. 1979, *Astr. Ap.*, **77**, 277.
Azzopardi, M. 1981, in *Proc. ESO Workshop on The Most Massive Stars*, ed. S. D'Odorico, D. Baade, and K. Kjär (Garching: European Southern Observatory), p. 227.
Azzopardi, M., and Vigneau, J. 1975, *Astr. Ap. Suppl.*, **22**, 285.
Butler, C. J. 1976, *Astr. Ap. Suppl.*, **24**, 299.
Caldwell, J. A. R. 1983, *Observatory*, **103**, 244.
Caldwell, J. A. R., and Coulson, I. M. 1984, *So. Africa Astr. Obs. Circ.*, **8**, 1.
———. 1985, *So. African Astr. Obs.*, preprint No. 370.
———. 1986, *M.N.R.A.S.*, **218**, in press.
Cohen, J. G. 1984, *A.J.*, **89**, 1779.
Feast, M. W., Thackeray, A. D., and Wesselink, A. J. 1960, *M.N.R.A.S.*, **121**, 337.
Feast, M. W., and Whitelock, P. A. 1984, *Observatory*, **104**, 193.
Florsch, A., Marcout, J., and Fleck, E. 1981, *Astr. Ap.*, **96**, 158.
Gascoigne, S. C. B., 1969, *M.N.R.A.S.*, **146**, 1.
Gascoigne, S. C. B., and Shobbrook, R. R. 1978, *Proc. Astr. Soc. Australia*, **3**, 285.
Graham, J. A., 1982, *Pub. A.S.P.*, **94**, 244.
Hodge, P. W., 1974, *Pub. A.S.P.*, **86**, 263.
Kraft, R. P., and Schmidt, M. 1963, *Ap. J.*, **137**, 249.
Martin, W. L., Warren, P. R., and Feast, M. W. 1979, *M.N.R.A.S.*, **188**, 139.
Martin, W. L. 1980, Ph.D. thesis, University of Cape Town.
Mathewson, D. S. 1984, *Mercury*, **13**, 57.
Mathewson, D. S., and Ford, V. L. 1984, in *IAU Symposium 108, Structure and Evolution of the Magellanic Clouds*, ed. S. van der Bergh and K. de Boer (Dordrecht: Reidel), p. 125.
———. 1985, in preparation.
McGonegal, R., McAlary, C. W., McLaren, R. A., and Madore, B. F., 1983, *Ap. J.*, **269**, 641.
McGonegal, R., McLaren, R. A., McAlary, C. W., and Madore, B. F. 1982, *Ap. J. (Letters)*, **257**, L33.
Murai, T., and Fujimoto, M. 1980, *Pub. Astr. Soc. Japan*, **32**, 581.
Payne-Gaposchkin, C., and Gaposchkin, S. 1966, *Smithsonian Contr. Ap.*, **9**, 1.
Sanduleak, N. 1968, *A.J.*, **73**, 246.
Sanford, R. F. 1956, *Ap. J.*, **123**, 201.
Thackeray, A. D. 1978, *M.N.R.A.S.*, **184**, 699.
Tully, R. B., and Wolff, S. C. 1984, *Ap. J.*, **281**, 67.
Visvanathan, N. 1983, *Ap. J.*, **275**, 430.
———. 1985, *Ap. J.*, **288**, 182.
Vogt, N., Geisse, H. S., and Rofas, S. 1981, *Astr. Ap. Suppl.*, **46**, 7.
Wallerstein, G. 1984, *A.J.*, **89**, 1705.
———. 1985, private communication.
Welch, D. L., and Madore, B. F. 1984, in *IAU Symposium 108, Structure and Evolution of the Magellanic Clouds*, ed. S. van der Bergh and K. de Boer (Dordrecht: Reidel), p. 221.
Wisniewski, W. Z., and Johnson, H. L. 1968, *Comm. Lunar and Planet. Lab.*, No. 112.

V. L. FORD, D. S. MATHEWSON, and N. VISVANATHAN: Mount Stromlo and Siding Spring Observatories, Private Bag, Woden, P.O. ACT 2606, Australia